JOINT PATTERNS IN THE MINERAL MOUNTAINS INTRUSIVE COMPLEX AND THEIR ROLES IN SUBSEQUENT DEFORMATION AND MAGMATISM

by John M. Bartley

Department of Geology and Geophysics, University of Utah, Salt Lake City, Utah

Link to supplemental data download: https://ugspub.nr.utah.gov/publications/misc_pubs/mp-169/mp-169-c.zip
Appendix

Miscellaneous Publication 169-C
Utah Geological Survey
a division of
UTAH DEPARTMENT OF NATURAL RESOURCES

This paper is part of *Geothermal Characteristics of the Roosevelt Hot Springs System and Adjacent FORGE EGS Site, Milford, Utah*. https://doi.org/10.34191/MP-169

Bibliographic citation:

Bartley, J.M., 2019, Joint patterns in the Mineral Mountains intrusive complex and their roles in subsequent deformation and magmatism, *in* Allis, R., and Moore, J.N., editors, Geothermal characteristics of the Roosevelt Hot Springs system and adjacent FORGE EGS site, Milford, Utah: Utah Geological Survey Miscellaneous Publication 169-C, 13 p., 1 appendix, https://doi.org/10.34191/MP-169-C.

JOINT PATTERNS IN THE MINERAL MOUNTAINS INTRUSIVE COMPLEX AND THEIR ROLES IN SUBSEQUENT DEFORMATION AND MAGMATISM

by John M. Bartley

ABSTRACT

Granitic rocks intersected by drill holes in the Utah FORGE site in Milford Valley strongly resemble the Oligocene-Miocene Mineral Mountains batholith and belong to the same structural block as the Mineral Mountains. Thus, the Mineral Mountains batholith and the FORGE reservoir may share the same joint pattern. Fractures in the Mineral Mountains plutonic complex were mapped in seven 0.03–0.08 km^2 areas in the northern half of the range to document orientations, spacing, continuity, intersection relationships, and orientations of slickenlines where present. To compare the patterns to those in the granitic rocks, fractures also were measured in four Pleistocene rhyolite bodies.

Fractures in batholithic rocks exposed near the FORGE area consist of three main sets: 1) strike ~090–110, dip 70°–90°; 2) strike ~010–040, dip 70°–90°; and 3) strike ~180±30, dip 30°±30° toward the west. All three sets formed either before or early during Basin-Range faulting. Slickenlines are sparse and mainly found on gently W-dipping set 3 fractures. Riedel shears consistently indicate top-west slip. Fracture patterns in the Pleistocene rhyolites differ both from those in adjacent granitic rocks and from one body to another, indicating that they reflect local near-surface stresses and are unrelated to deeper joint patterns.

Fracture sets 2 and 3 are inferred to be a conjugate set formed with a vertical maximum compressive stress, followed by ~40° eastward tilt. Eastward tilting of the range is indicated by a) the wall-rock map pattern; b) eastward dips of stratified rocks exposed in the range; c) late Miocene dikes that dip 40°–50° west but probably were originally vertical; and d) paleomagnetic data that, although too scattered to reliably quantify the magnitude, indicate eastward tilt of the plutonic complex. The lack of evidence for a large-offset W-dipping normal fault on the east side of the Mineral Mountains favors the isostatic rolling-hinge mechanism for tilting, which implies that the range tilted as it was unroofed by faulting.

The fracture pattern in the batholith and other evidence suggest three further implications. First, the average orientation of slipped joints in the range parallels the bedrock-basin fill contact which most authors have interpreted to be the basin-bounding fault. This suggests that the basin-bounding fault developed by shear across set 3 fractures. Second, the NNE-striking Opal Mound fault strikes subparallel to steep N-striking set 2 fractures and probably represents shear across that fracture set. The rolling-hinge mechanism predicts this shear sense in the footwall of the basin-bounding fault, and therefore the Opal Mound fault may reflect isostatic rebound of the footwall as it was unroofed by faulting. Finally, the WNW-striking Negro Mag fault probably formed by shear across steep E-striking fractures of set 1. Geomorphic evidence suggests south-side-up displacement across the fault, and the majority of Pleistocene rhyolitic volcanism in the range is located on the upthrown side. These relations suggest the hypothesis that the Negro Mag fault is the northern boundary of a bysmalith (i.e., fault-bounded laccolith) that formed part of the shallow magmatic plumbing system during Pleistocene magmatism. This further suggests that, although the youngest intrusive rocks exposed at the surface are Miocene in age, growth of the batholith continued into the Pleistocene and may be presently ongoing.

INTRODUCTION

The Utah FORGE site is located near the eastern edge of Milford Valley, a basin formed by late Cenozoic crustal extension at the eastern margin of the Basin and Range Province (Figure 1). Because basin-filling sediment conceals the granitic bedrock of the FORGE enhanced geothermal system (EGS) reservoir, geologic questions that are important to the FORGE project include 1) what is the relationship between granitic rocks intersected by drill holes in and near the FORGE site to the bedrock exposed in the surrounding ranges, and 2) to what extent can observed characteristics of the exposed bedrock be used to predict characteristics in the FORGE EGS reservoir?

The Mineral Mountains form the eastern boundary of the Milford Valley basin and provide the bedrock exposures nearest to the FORGE site (Figure 1). The Mineral Mountains are dominated by an Oligocene-Miocene granitic batholith, and granitic rocks intersected by drill holes in Milford Valley almost certainly belong to the same intrusive complex. Seismic imaging (Smith and

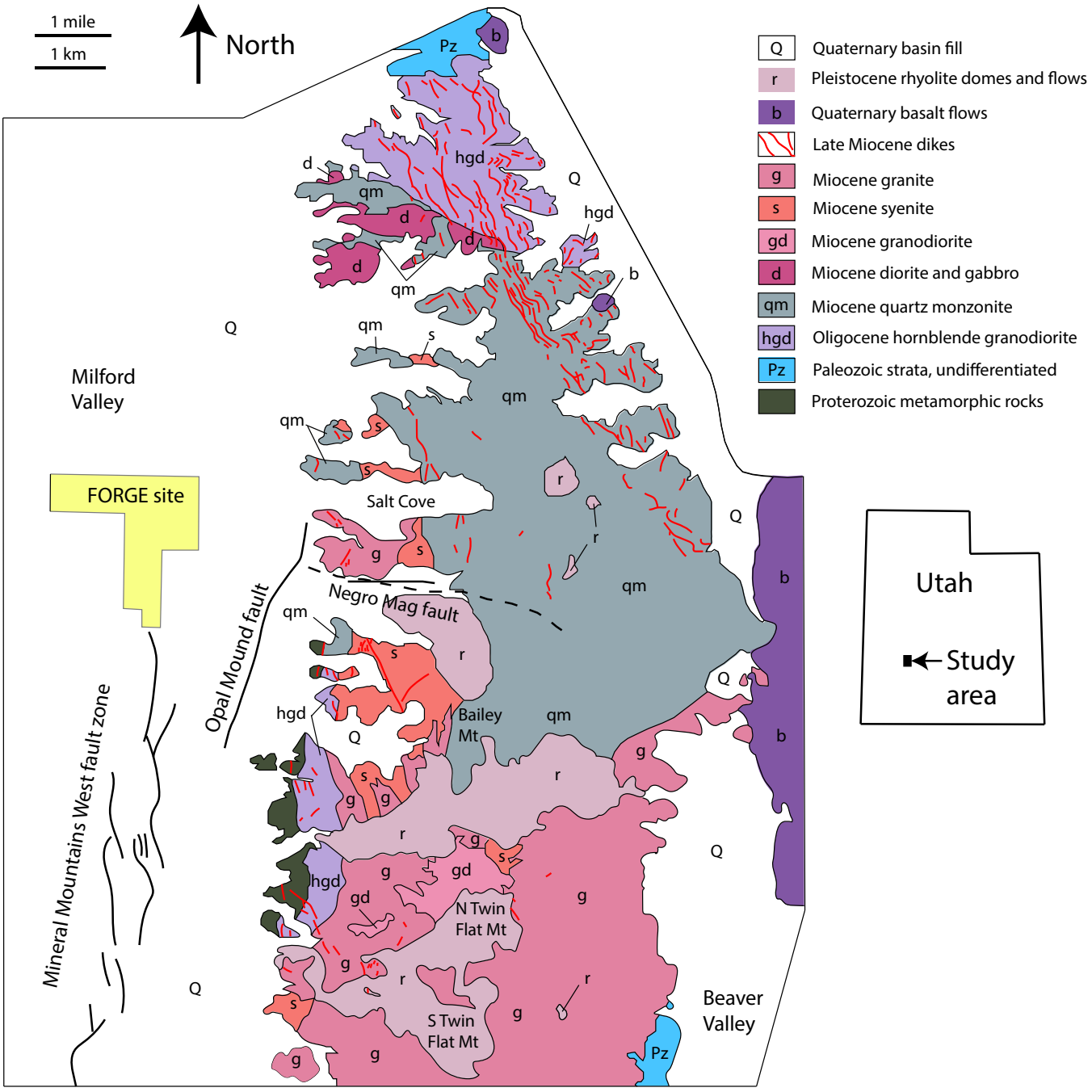

Figure 1. *Generalized geology of the north-central Mineral Mountains, simplified from Sibbett and Nielson (2017).*

Bruhn, 1984; Nielson et al., 1986; Miller et al., 2019) and inversion of gravity data (Hardwick et al., 2019) indicate that the basin fill-bedrock contact at the eastern margin of Milford Valley dips ~30° to the west. Previous investigations (e.g., Smith and Bruhn, 1984; Nielson et al., 1986; Coleman et al., 1997) interpreted the basin fill-bedrock surface to be a west-dipping normal fault that formed the Milford Valley basin. Miller et al. (2019) interpret new, more detailed seismic imaging to indicate erosion of the bedrock surface before its burial. Other evidence noted by earlier studies nonetheless favors formation of the basin by a west-dipping master fault. For example, the most likely explanation for exposure of Proterozoic basement at the western foot of the Mineral Mountains is that it was unroofed in the footwall of a major west-dipping normal fault. Practically all other outcrops of Proterozoic basement in Utah, including the Beaver Dam Mountains, Wasatch Range, Grouse Creek Mountains, Raft River Mountains, and Antelope Island, are exposed in the footwalls of major normal faults (Hintze et al., 2000). Therefore, the basin fill-bedrock contact in the FORGE area may nonetheless represent the basin-bounding fault, but the fault surface was exposed and modified by erosion before its current complete burial by basin fill. Observations of fractures in the Mineral Mountains reported here are consistent with interpretation of the basin fill-bedrock contact as a west-dipping normal fault, and this interpretation

places granitic rocks in the FORGE area in the same major structural block as the Mineral Mountains. This in turn implies that field observations of granitic rocks exposed in the Mineral Mountains are apt to be useful in predicting properties of granitic rocks in the FORGE area.

Methods

Three types of structural data were collected:

1) Fracture orientations, with kinematic information where available along fractures that accommodated shear displacement. The complete fracture data set is presented in the Appendix[1] to this report.

2) Detailed fracture maps (resolution ~1 m) of small areas (0.03–0.08 km^2) of excellent exposure to document fracture lengths and continuity and their intersection relationships.

3) Field photographs to portray geometric relations of gently dipping fractures which tend to be inadequately represented by a conventional horizontal map.

All data types were collected simultaneously during mapping. The relative abundances of fractures in different sets may thus be portrayed less precisely than achievable by more objective sampling (e.g., measuring all fractures along a scanline). The importance of the other data types justifies this compromise. Reconnaissance fracture orientation data also were collected in some locations where fractures were not mapped.

Study Areas

Seven areas of exceptional exposure were mapped, in Oligocene hornblende granodiorite (1 area), Miocene quartz monzonite (4 areas), Miocene granite (1 area), and Miocene syenite (1 area). The Oligocene granodiorite is more intensely fractured and faulted than any of the Miocene granitic rocks. This may reflect early Miocene deformation that is recorded by an angular unconformity between late Oligocene and Miocene stratified rocks exposed at the southern end of the range (Price, 1998). In order to compare the fracture patterns to those found in granitic rocks, fractures also were measured in four Quaternary rhyolite bodies including the Bailey Ridge lava flow, a lava dome on the southwest flank of Bailey Mountain, and the lava domes that form North and South Twin Flat Mountains.

Fracture and Fault Data

Fracture Spacing

There is an overall northward trend of decreasing fracture spacing in the Miocene plutonic rocks (Figure 2). Fracture spacing also varies somewhat with rock type (Figure 3A). Miocene granitic rocks generally contain the sparsest macroscopic fractures, and this does not appear to vary from granite to quartz monzonite to syenite. The Oligocene granodiorite is more intensely fractured and appears to be significantly more deformed than adjacent Miocene granitic rocks. Closely spaced fractures likely contributed to the fact that only one outcrop area of Oligocene granodiorite provided sufficiently continuous exposure to undertake fracture mapping. Silicic dikes, including both aplite dikes that are cogenetic with batholithic rocks and post-batholith rhyolite dikes, are by far the most intensely fractured rocks in the range. Fracture spacings of 10 cm or less are common in the silicic dikes, making mapping fractures at the ~1:1000 scale used in this study clearly impractical.

Fracture Orientations and Continuity

Although the fracture intensity varies, Miocene granitic rocks in the northern half of the range all contain a similar fracture pattern (Figure 4). The pattern includes three fracture sets in the following general orientations: 1) strike ~090–110, dip 70°–90°; 2) strike ~010–040, dip 70°–90°; and 3) strike ~180±30, dip 30°±30° toward the west. In some stereoplots, two of the concentrations of poles to fractures that define the three sets merge into a girdle, but the overall pattern remains much the same.

The relative abundances and continuity of the three main fracture sets in the northern part of the range vary considerably (Figure 5). Set 2 fractures that strike from north to northeast and dip steeply NW and SE dominate in Miocene quartz monzonite exposures near the northern end of the range. In the central map areas that are located nearest to the FORGE area, steep E-W striking fractures of set 1 are more abundant and continuous. In these areas, the steep E-W fractures of set 1

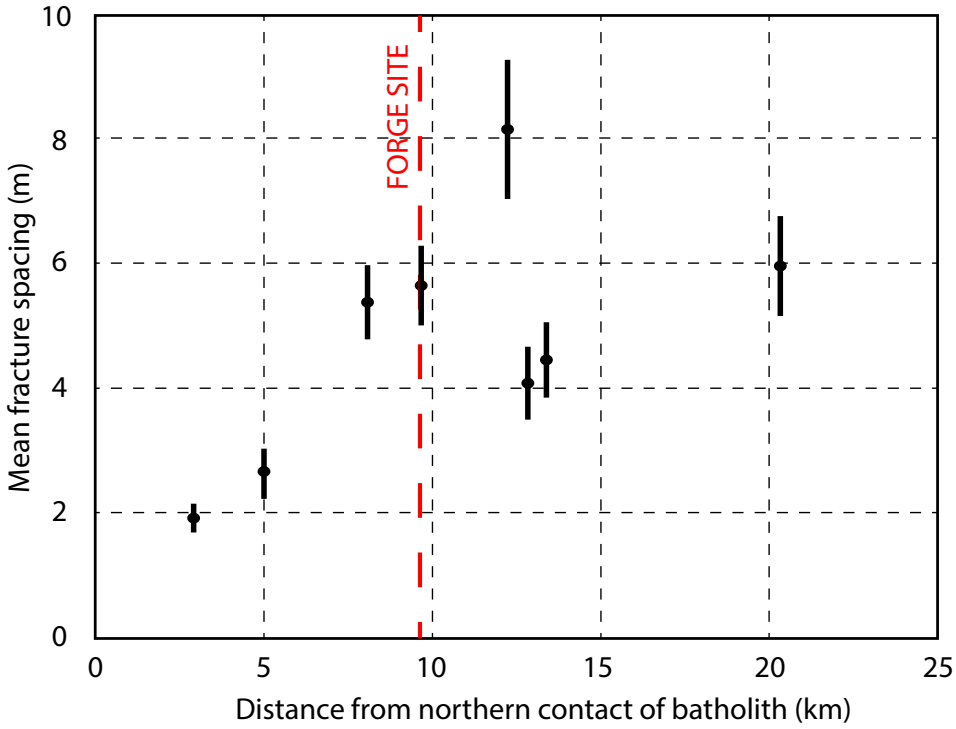

Figure 2. *Fracture spacing vs. location along the range. Fracture spacing was determined by counting mapped fractures intersected by scan lines 50–100 m in length and oriented 000°, 030°, 060°, 090°, 120°, and 150°. Three scan lines in each orientation were placed at arbitrary locations on each fracture map. Error bars are 1σ based on reproducibility of fracture counts.*

commonly bound fractures belonging to sets 2 and 3, and set 3 fractures commonly have N-S extents of only tens of meters (Figure 2B). In the southern area shown in Figure 5, gently west-dipping set 3 fractures are more abundant and longer than in the other areas shown.

Fracture sets 2 and 3 are interpreted to represent a conjugate set (Figure 2C). The fracture geometry illustrated by Figure 2C is prominent in all study areas from Salt Cove southward. As indicated in the figure, the geometry is interpreted to have formed with the maximum compressive stress vertical, as predicted for the normal fault regime in the Anderson fault theory (Anderson, 1951), followed by ~40° of west-side-up (eastward) tilt in the footwall of the normal fault that formed Milford Valley. This implies that the conjugate set formed before large displacement had accumulated across the basin-bounding fault, which probably began in late Miocene time (Coleman et al., 2001). Because fracture intersection relationships indicate that the conjugate set formed after the E-W steep fractures, all three main fracture sets appear to have formed before or early during Basin-Range faulting, and therefore in the middle Miocene shortly after the batholith was emplaced.

Several lines of evidence confirm that the Mineral Mountains block has been tilted. First, the only exposures of Proterozoic basement in the region are located on the western flank of the Mineral Mountains and, passing eastward from there, progressively shallower crustal levels are exposed, culminating in the flat-lying Cenozoic volcanic rocks that form the next range to the east, the Tushar Mountains. Second, stratified rocks in the Mineral Mountains all dip to the east. Most significant are Oligocene and Miocene strata exposed at the southern end of the range that dip from 30° to 80° eastward (Price, 1998). Third, a swarm of felsic and mafic dikes dated at 11 Ma (Coleman and Walker, 1994) is widespread in the range but is particularly prominent in the northern approximately one-third of the batholith (Figure 1). The dikes consistently dip moderately (40°–50°) westward and, if originally emplaced vertically, imply 40°–50° of eastward tilt since 11 Ma. Fourth, paleomagnetic data from Cenozoic intrusive rocks, although of uneven quality, suggest 30°–90° of eastward tilting of much of the range (Coleman, 1991).

Fracture patterns in the Pleistocene rhyolite domes and flows bear little resemblance to fracture patterns in nearby exposures of granitic rocks (Figure 6). Steep fractures predominate in all of the rhyolite bodies, but otherwise there are few similarities from one body to another. The predominance of a single fracture set in the South Twin Flat dome suggests a minimum horizontal stress trajectory along an azimuth of 045°, roughly orthogonal to in situ stress orientation inferred from hydrofracture in drill hole 58-32. Fracture patterns in the other three rhyolite bodies are more complex and not easily interpreted in terms of in situ stress. Because the rhyolite fracture patterns differ from each other as well as from patterns in the underlying granitic rocks, the fractures are inferred to reflect local near-surface stresses that are not relevant to either fracture patterns or the state of stress at depth.

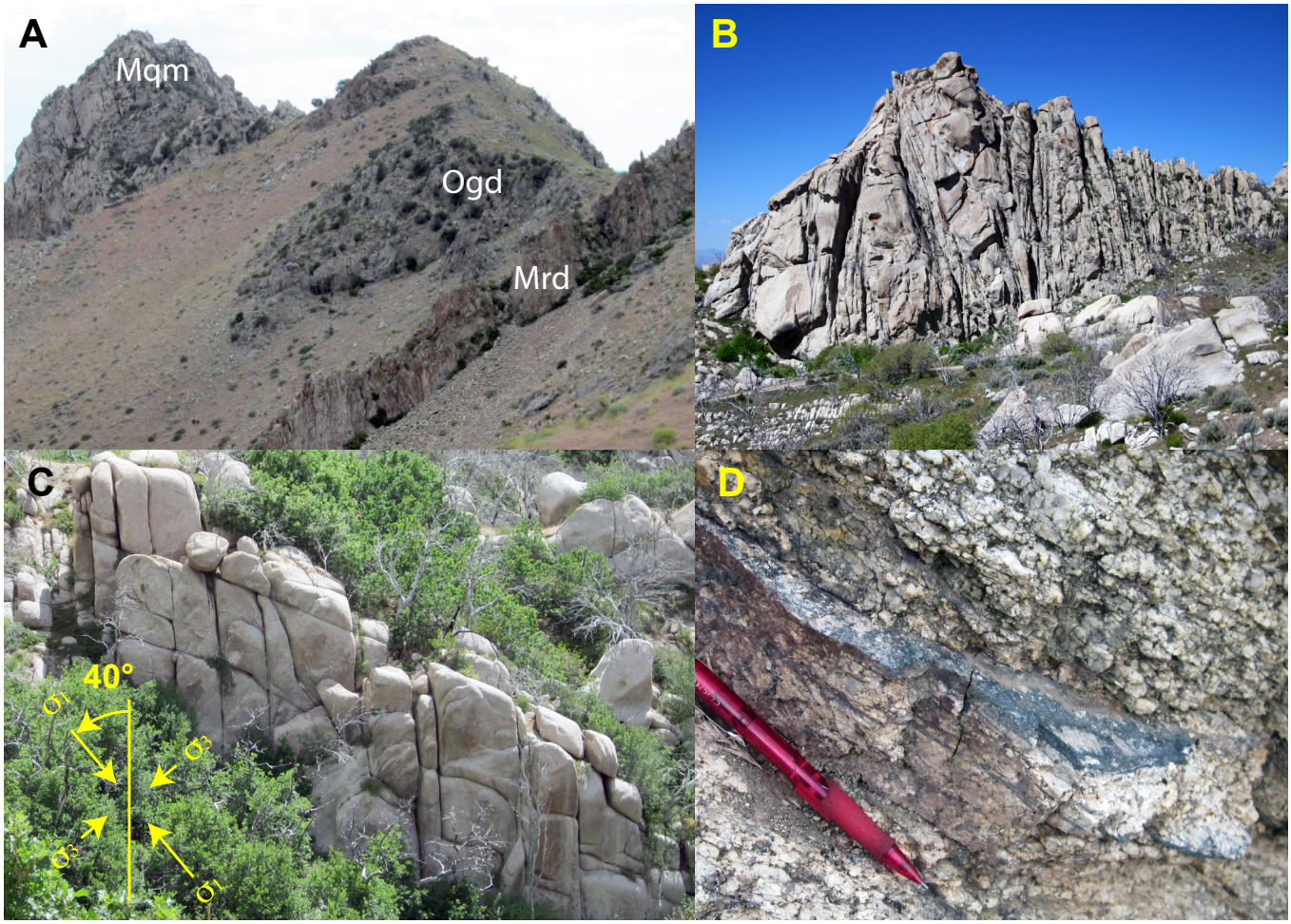

Figure 3. *Field photographs of fractures and fracture patterns in the Mineral Mountains.* ***(A)*** *Distant view of ridge crest northwest of Pinnacle Pass; note massive jointing of Miocene quartz monzonite (Mqm), intense jointing of Miocene rhyolite dike (Mrd), and intermediate joint density in Oligocene granodiorite (Ogd).* ***(B)*** *View westward along strike of E-W subvertical joints, Salt Cove map area. Note that gently dipping joints terminate against subvertical joints. The steep joints are interpreted to be older than, and to have been barriers to the propagation of, the gently west-dipping joint set.* ***(C)*** *View southward approximately along the strike of subvertical N to NE-striking joints and gently west-dipping joints. Based on their geometry and on independent evidence for eastward tilting of the range, these two joint sets are interpreted to be a tilted conjugate set. The conjugate set probably formed with σ1 (maximum compressive stress) vertical (i.e., normal fault stress regime) and subsequently the joints were tilted 40° eastward to their present orientations.* ***(D)*** *Cataclasite with dark greenish (probably chloritic) matrix formed by shear displacement across a west-dipping joint. Similar cataclasite is found in fractures in a variety of orientations, but mostly commonly in fractures that dip broadly westward at angles less than 40° (see Figure 5).*

Fault Geometry and Kinematics

Slickensided fault surfaces (Figures 3D, 7) are generally very sparse in the granitic rocks, with three exceptions. The Oligocene granodiorite at the northern end of the range contains numerous faults, including at least one meter-thick cataclastic zone that dips gently westward. The Miocene quartz monzonite where it is exposed on the northern wall of Negro Mag Canyon contains numerous thin (1–5 cm) cataclastic zones, as does syenite exposed on the western slopes of Bailey Mountain.

Although fractures that show evidence of shear displacement range in orientation, the majority dip gently to moderately westward with highly variable strikes (Figure 7). The average orientation of slipped fractures, determined by applying Bingham statistics to the orientations of poles to the fractures, is (173°, 30°). Slickensides and Riedel shears consistently indicate top-to-the-west shear. Such fractures exposed in Negro Mag Canyon were interpreted to be map-scale low-angle faults by Sibbett and Nielson (2017). However, the present mapping indicates that they represent slip across joints that commonly are bounded by E-W striking steep fractures and thus have small N-S extents. It therefore appears unlikely that any of the low-angle faults exposed in Negro Mag Canyon are either continuous over large areas or accommodated tectonically significant displacements.

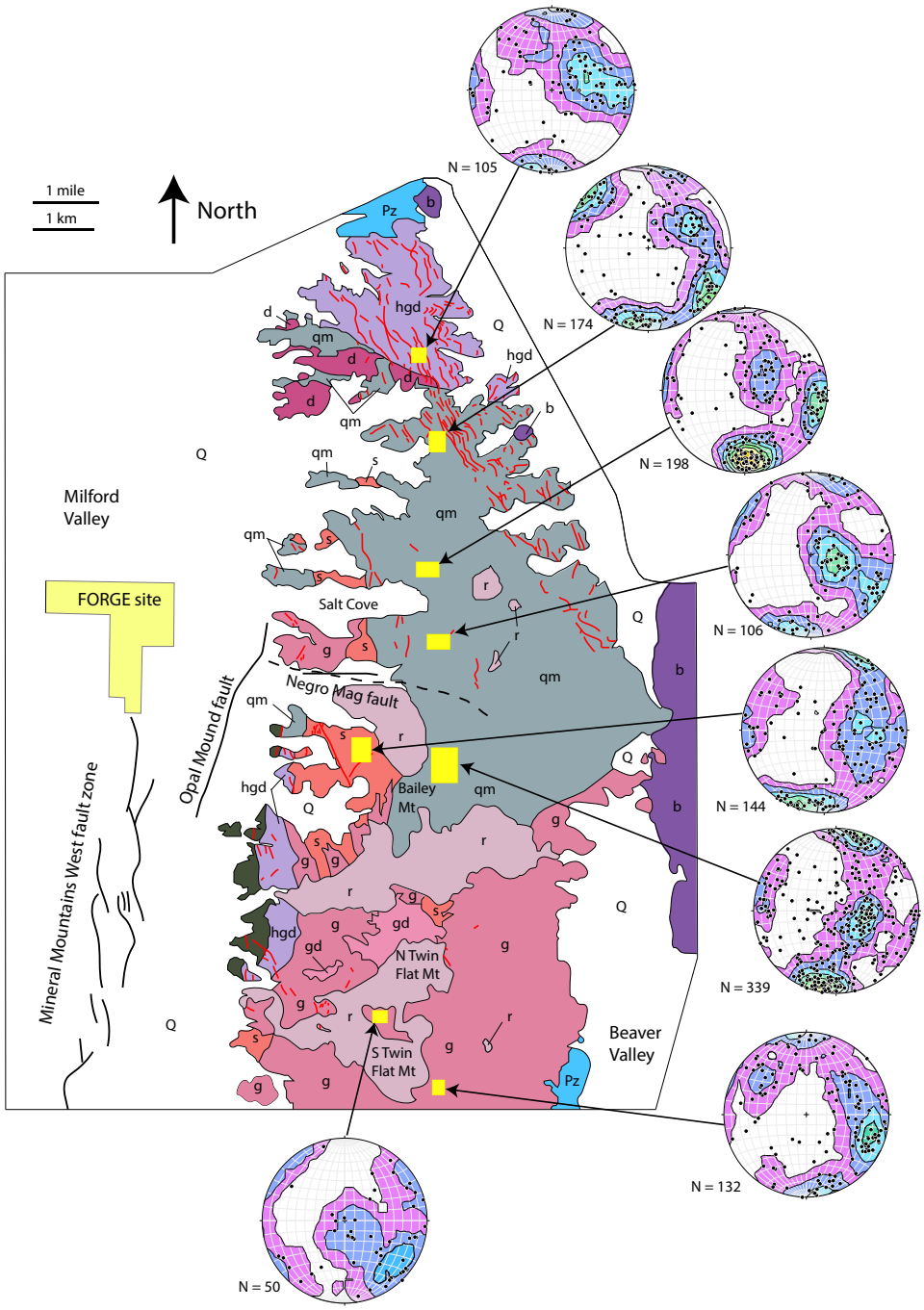

Figure 4. *Lower hemisphere equal-area stereoplots of poles to fractures in Oligocene and Miocene granitic rocks. These and all subsequent stereo plots are contoured using the Kamb (1959) method. See Appendix for data on which the plots are based. Base map is the same as Figure 1. Yellow squares are areas covered by present study. All stereoplots in this paper were constructed using Stereonet v. 10.*

Fracture Fillings

Fracture fillings are relatively uncommon in the study areas, although it is unclear to what extent this reflects fractures that remained open after formation versus removal of fillings by surface weathering. Where present, fillings are dominated by iron oxides, including both magnetite (based on deflection of a compass needle) and fine-grained hematite (based on its distinctive red color). The fillings occasionally are hard and resistant, probably indicative of silicification; this, however, is uncommon. Fillings have been observed in fractures belonging to all of the dominant sets, but are most common in set 1.

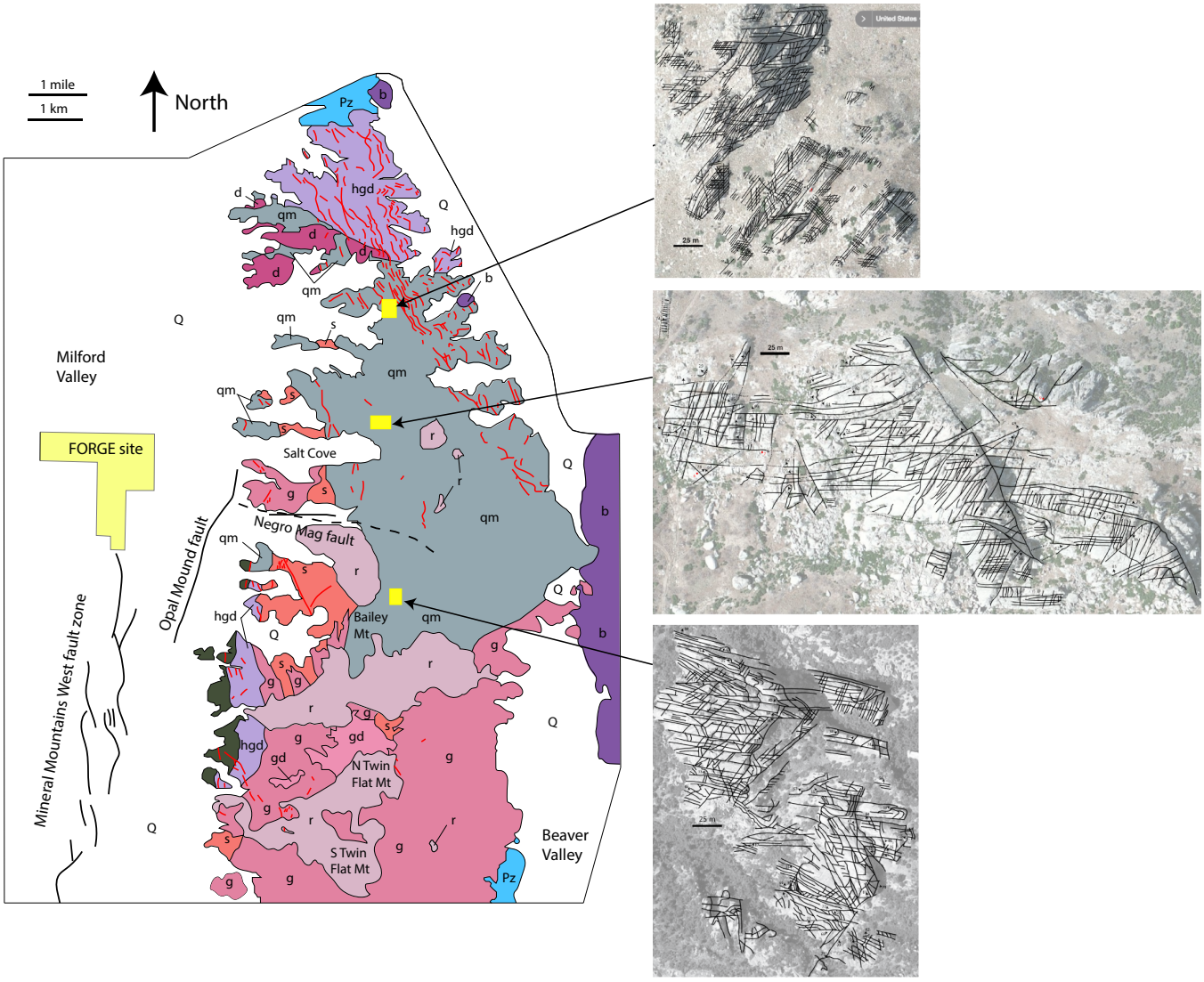

Figure 5. *Representative fracture maps, all plotted at the same scale. Photographic base was downloaded from Bing maps and is not orthorectified. Although all areas contain much the same fracture sets (Figure 4), their relative abundance and continuity vary greatly. In these examples, the northern area is dominated by steep broadly N- to NE-striking fractures of set 2; steep E-W striking fractures of set 1 are more prominent in the central (Salt Cove) area; and in the southern area, gently W-dipping fractures of set 3 (recognizable by their sinuous traces as well as measured dips) are longer and more prominent than in other areas.*

Discussion

Origin and Geometric Evolution of the Basin Boundary

Both seismic imaging and inversion of the gravity field indicate that the contact between basin fill and bedrock on the eastern side of Milford Valley dips ~30° to the west. Fracture data presented here are consistent with interpretation of that surface as the footwall side of the basin-bounding fault, perhaps somewhat modified by erosion after exposure by removal of the hanging wall (Miller et al., 2019). This dip is substantially lower than the expected 60° initial dip for a normal fault (Anderson, 1951), and lower than the 45° average dip inferred for active crustal-scale normal faults based on earthquake focal mechanisms (Thatcher and Hill, 1991). Smith and Bruhn (1984) and Nielson et al. (1986) posited a listric fault geometry (i.e., the fault dip decreases downward; e.g., Hamblin, 1965). However, observational confirmation of a listric geometry is lacking, and mechanical models for formation of listric normal faults in bedrock are problematic (e.g., Wills and Buck, 1997). In view of the abundant evidence that the range has been tilted eastward, it is more likely that the range-bounding fault formed at a high angle and has been tilted to its present orientation (Coleman and Walker, 1994; Coleman et al., 1997).

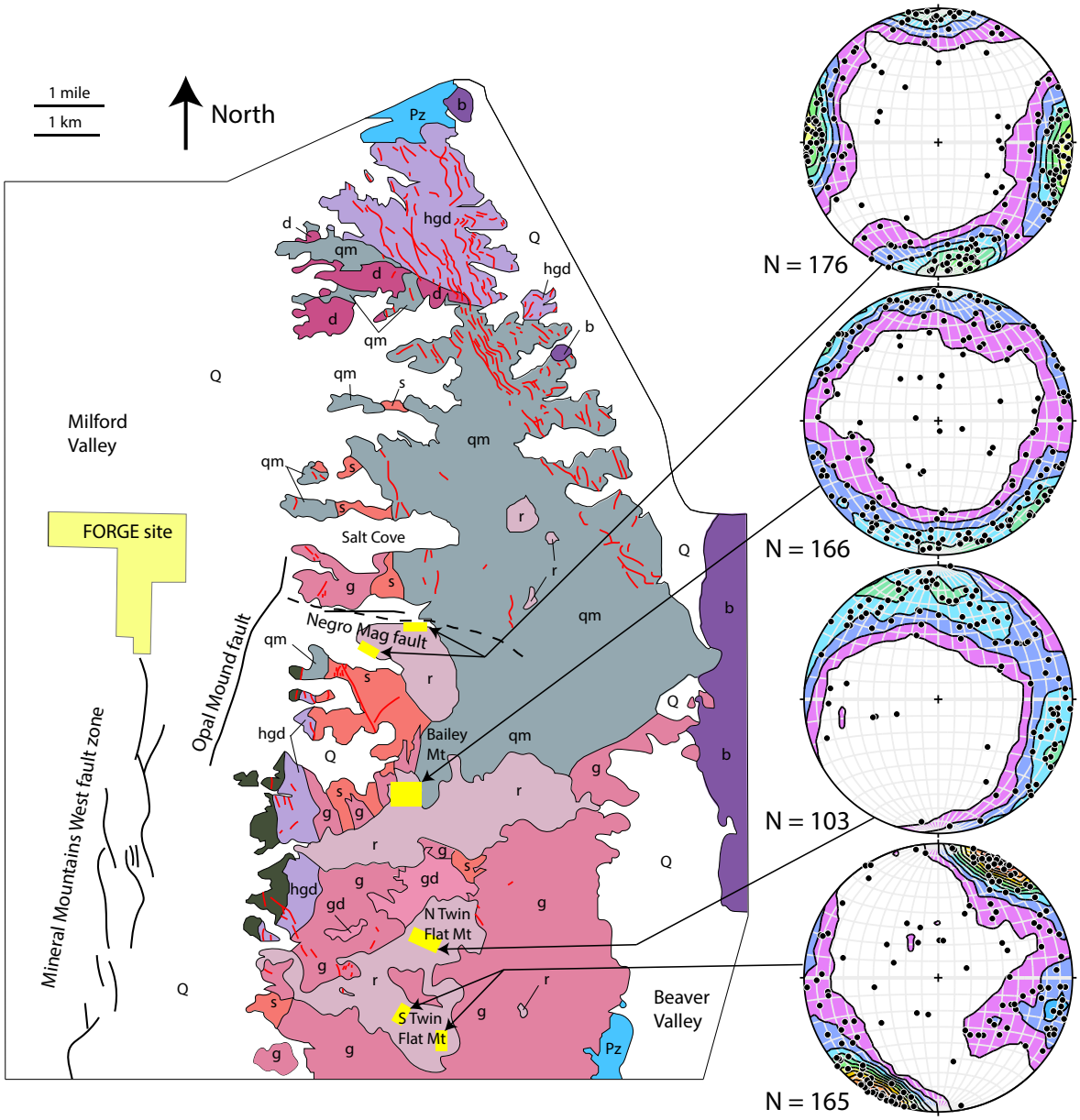

Figure 6. *Lower hemisphere equal-area stereoplots of poles to fractures in Pleistocene rhyolite domes and flows. Base map is the same as Figure 1. See Appendix for data on which the plots are based. Yellow squares are areas where fractures were measured. Note that steep fractures dominate all data sets, but that otherwise all of the patterns differ from each other. The patterns also bear little resemblance to the pattern seen in adjacent plutonic rocks (Figure 4).*

The conjugate pattern of fracture sets 2 and 3, combined with the independent evidence of eastward tilting, strongly suggests that the low-angle normal faults in the range formed as steeply west-dipping joints that during and/or after shear displacement were tilted to low dips, in rare instances through horizontal (Figure 7). The average orientation of the slipped joints (173°, 30°) is subparallel to the bedrock-basin fill surface. This suggests that the basin-bounding fault was initiated by shearing across set 3 fractures.

Tilting of the range and basin-bounding fault could have been achieved by several alternative mechanisms, including the domino model (tilting of an array of fault blocks between parallel normal faults; e.g., Proffett, 1977); reverse drag above an underlying listric normal fault (Coleman and Walker, 1994); or the rolling-hinge mechanism (isostatic upward flexure of a normal fault footwall; Spencer, 1984; Wernicke and Axen, 1988; Buck, 1988; Axen and Bartley, 1997). Both the domino model and reverse drag require a major west-dipping normal fault between the Mineral Mountains and the Tushar Mountains to the east. Whereas faults are certainly present in Beaver Valley (Machette et al., 1984), none has produced the large structural relief which would be required to significantly tilt the Mineral Mountains block. The absence of such a fault thus favors the rolling-hinge mechanism. Figure 8 schematically illustrates formation of Milford Valley and the Mineral Mountains according to the rolling-hinge model.

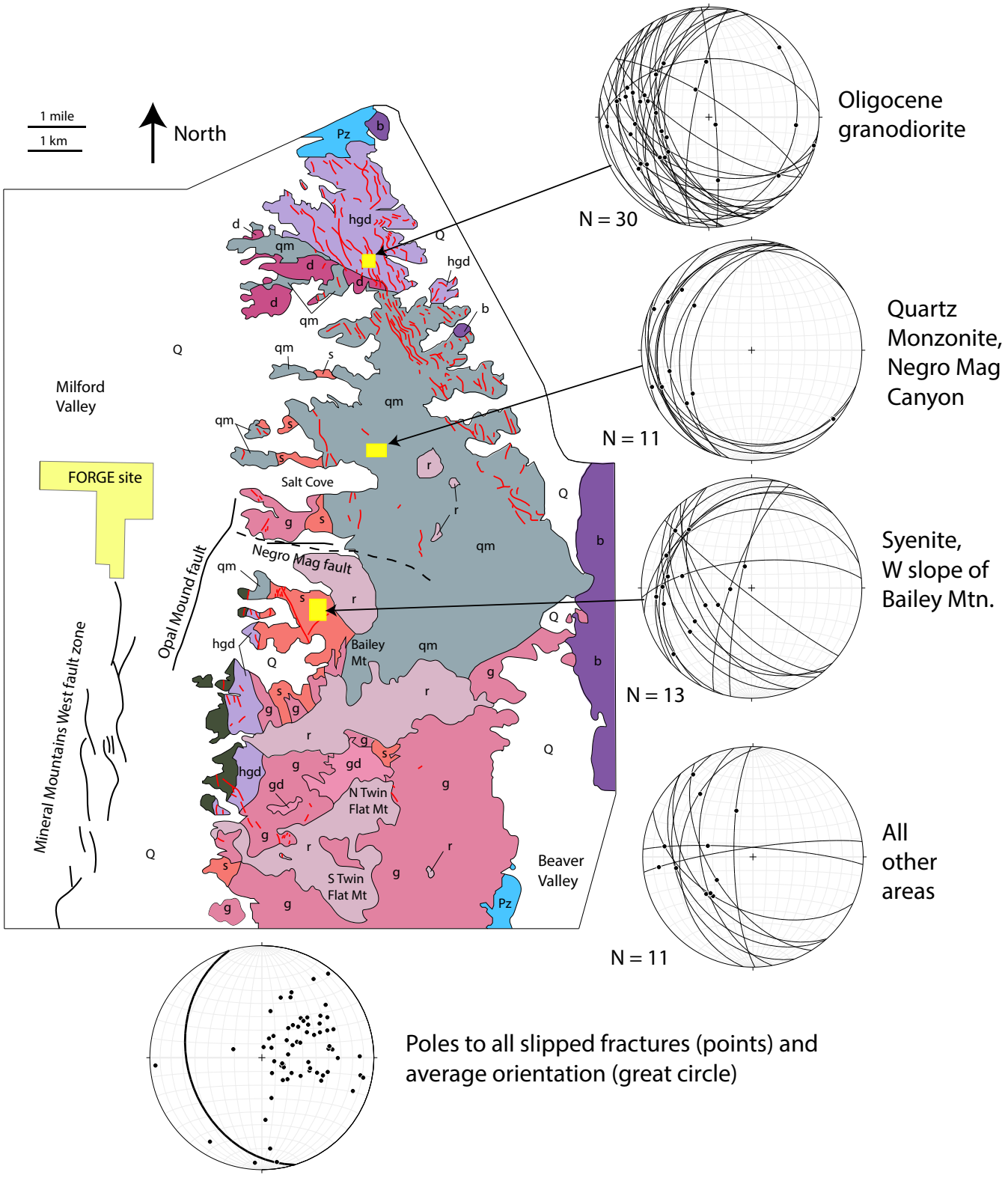

Figure 7. *Lower hemisphere equal-area stereoplots of fault kinematic data, located on the same base map as Figure 1. See Appendix for data on which the plots are based. In all but the bottom plot, great circles are fault planes. Points are slip directions based on slickenlines or, in three instances in which slickenlines were not visible, indicated by measured orientations of Riedel shears, assuming that the slip direction is normal to the intersection of Riedel shears with the fault plane. In the bottom plot, points are poles to all sheared fractures, and the great circle is their average orientation (173, 30) determined by Bingham statistical analysis in Stereonet v. 10.*

Surficial evidence of faulting at the range front is largely absent (Knudsen et al., 2019). Indications of a tectonically active range front such as fault scarps and faceted spurs are absent, and the range front is deeply embayed at drainages that issue from the range. However, the Mineral Mountains West fault zone (Figure 1; Knudsen et al., 2019) is defined by a north-trending system of fault scarps in Quaternary deposits. Along most of its length, the Mineral Mountains West fault zone is located ~2–3 km from the range front. However, south of Figure 1, the range front steps about 5 km to the west and, as a result, the fault zone and range front coincide. No offset of the bedrock surface under the basin has been detected beneath Mineral Mountains West fault scarps, yet seismic rupture of a magnitude sufficient to form surface scarps implies slip across a surface with a down-dip extent of several kilometers. Therefore, the most likely interpretation is that the Mineral Mountains West fault zone roots into the fault that forms the basin fill-bedrock contact, which therefore underwent seismic slip down-dip from where the scarp-forming fractures intersect the bedrock surface. The general lack of evidence for active faulting at the range front implies that the shallow part of the basin-forming fault that lies to the east of the Mineral Mountains West fault zone has been abandoned, as predicted by the rolling-hinge model (Figure 8).

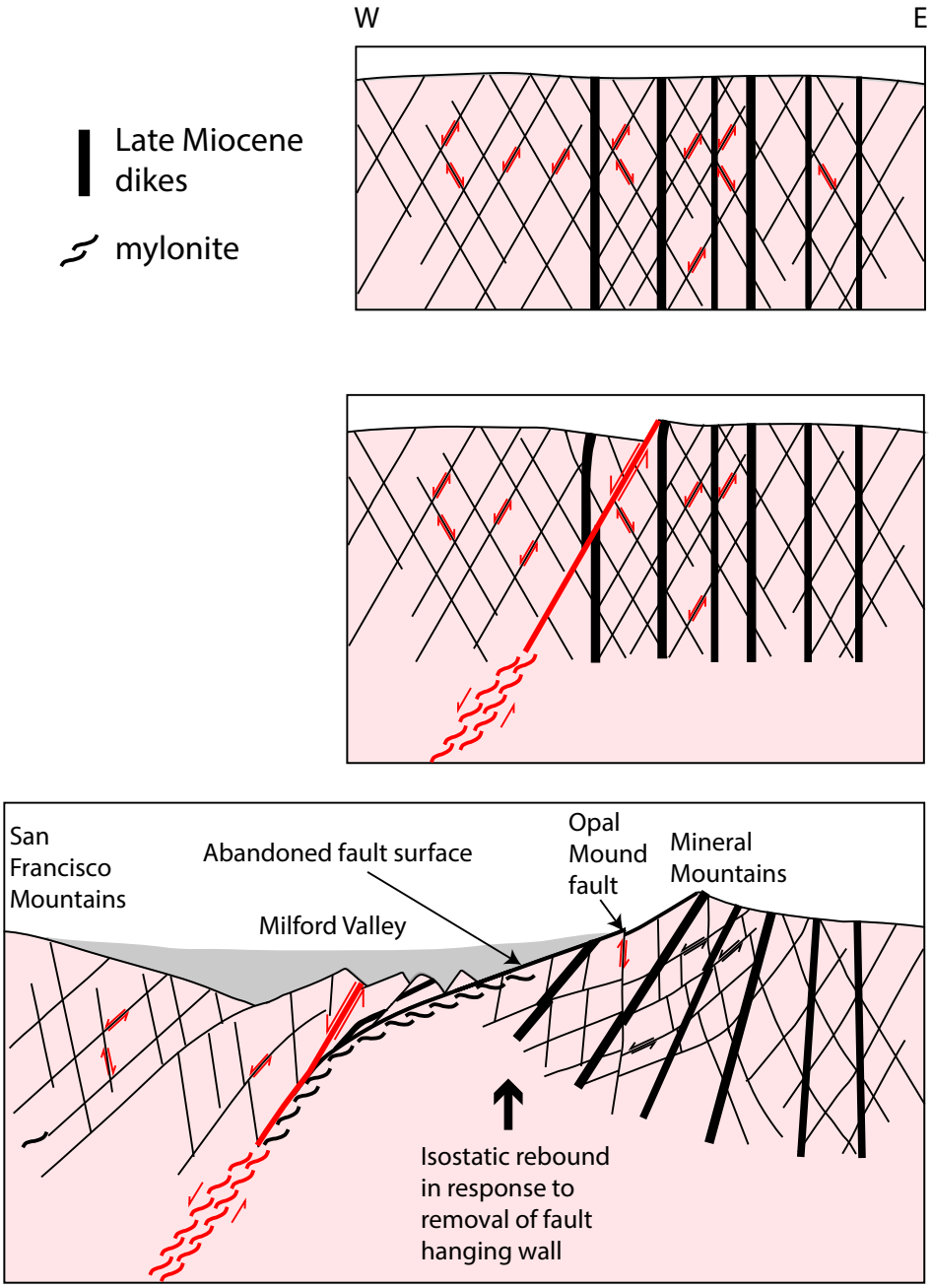

Figure 8. *Schematic east-west profiles (not to scale) illustrating orientations of the dike swarm and joint sets 2 and 3; nucleation of the basin-bounding fault on joint set 3; and fault displacement to form Milford Valley, with tilting driven by isostatic adjustment to removal of the hanging wall of the fault.*

Opal Mound Fault

The Opal Mound fault (Figure 1) is oriented similarly to steep NNE-striking fractures of set 2 within the range. Therefore, like the basin-bounding fault, the Opal Mound fault probably formed by shear across a pre-existing joint set. Surficial geology indicates west-side-up movement (Knudsen et al., 2019). This shear sense across the Opal Mound fault could be driven by the same isostatic forces that cause the geometry of the basin-bounding normal fault to evolve according to the rolling-hinge mechanism (Figure 8). Geometrically similar faulting in the footwalls of other large-displacement normal faults has been interpreted to reflect rolling-hinge deformation (e.g., central Mojave metamorphic core complex, Bartley et al., 1990; Raft River Mountains, Manning and Bartley, 1994; Tauern window in the Austrian Alps, Axen et al., 1995).

Negro Mag Fault

The Negro Mag fault also appears to reflect shear across a fracture set in the batholith, in this case the steep, broadly E-striking fractures of set 1. Geomorphic evidence suggests south-side-up displacement (Knudsen et al., 2019). Nearly all of the Pleistocene rhyolite bodies are located south of the Negro Mag fault and thus on its upthrown side. These observations suggest that motion across the Negro Mag fault may be linked to, and perhaps even driven by, Pleistocene rhyolitic magmatism.

Figure 9 illustrates one hypothesis for such a link. A bysmalith (also sometimes called a punched laccolith) is a subhorizontal tabular intrusion, space for which is made by uplift of a fault-bounded roof block. In Figure 9, the Negro Mag fault is inferred to be the northern boundary of such a roof block that would likely include all of the area characterized by Pleistocene rhyolite extrusions. No location is proposed here for the rest of the boundary of the uplifted block implied by this hypothesis. The boundaries of the uplifted roof block would be inherently difficult to locate in the massive granitic rocks that characterize most of the range, and the western and eastern boundaries could be concealed by recent sedimentation. The location and orientation of the Opal Mound fault invite speculation that it might be related to recent magma intrusion at depth, but its west-side-up offset is inconsistent with this suggestion. The Mineral Mountains West fault zone has the expected sense of offset, but the lack of offset of the basin fill-bedrock contact is difficult to reconcile with a relationship to magma intrusion under the range. As noted above, it is more likely that the Mineral Mountains West fault zone defines the up-dip limit of the most recent displacement across the basin-bounding fault.

If the bysmalith hypothesis is correct, it carries with it a broader implication for the nature and duration of batholith growth. Recent detailed geochronology of well-exposed intrusive complexes indicates that granitic plutons typically grow incrementally downward (e.g., Coleman et al., 2004; Michel et al., 2008). This implies that the age range of exposed batholithic rocks may encompass only part of the construction of the intrusive complex, and that it is particularly likely for the youngest components of an intrusive complex to remain unexposed in the subsurface. The hypothetical Pleistocene bysmalith would constitute such a younger, as-yet unexposed addition to the batholith. Although the youngest intrusive rocks presently exposed at the surface are Miocene in age, growth of the Mineral Mountains batholith may have continued into the Pleistocene, and the presence of an active high-temperature geothermal system suggests that growth of the Mineral Mountains batholith even may be ongoing.

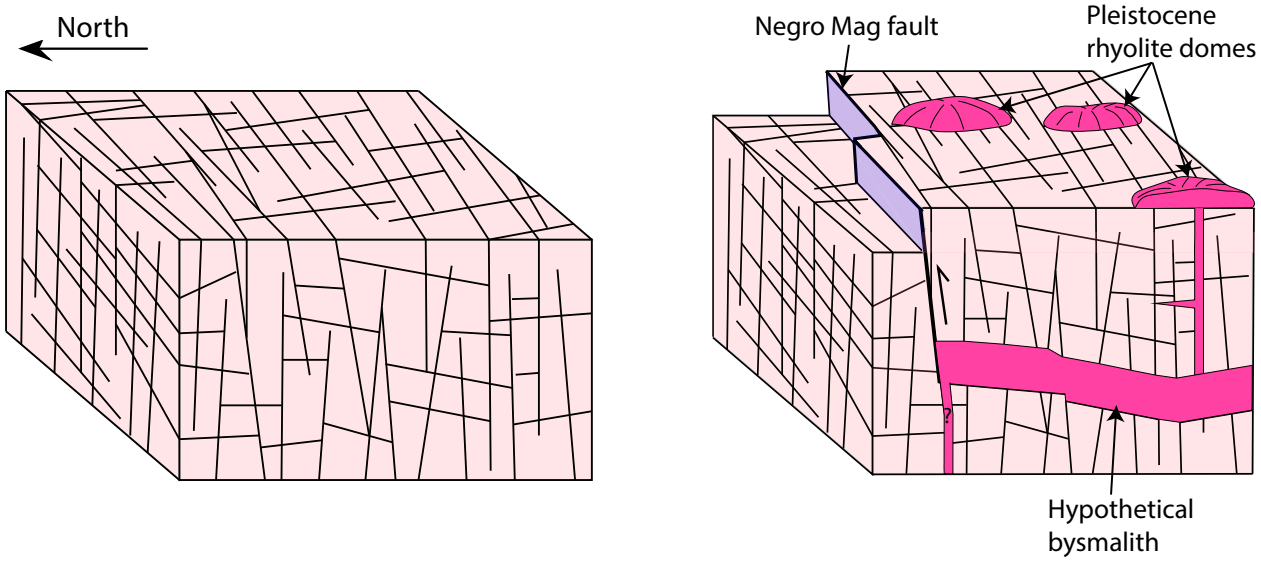

Figure 9. *Cartoon block diagram illustrating hypothetical interpretation of the Negro Mag fault as the northern boundary of a bysmalith that underlies the Pleistocene rhyolitic volcanic field.*

CONCLUSION

Miocene granitic rocks near the Utah FORGE site contain three dominant joint sets in the following orientations: 1) strike ~100±10°, dip 70°–90°; 2) strike ~025±25°, dip 70°–90°; and 3) strike ~180±30°, dip 30°±30° toward the west. Sets 2 and 3 are interpreted to form a conjugate set that formed prior to or early during Basin and Range extension. The batholith, the joints that it contains, and the west-dipping normal fault that bounds the Milford Valley basin all underwent ~40° of west-side-up tilt during Basin and Range extension. The tilting is interpreted to reflect isostatic rebound during unroofing of the range by the basin-bounding fault (rolling hinge mechanism). Each of the three significant faults in the vicinity of the FORGE site is oriented subparallel to one of the main joint sets and probably was initiated by shear across joints of that set. Most of the joints in the range that have been sheared belong to set 3. The average orientation of the sheared joints is subparallel to the basin-bounding fault, which thus is interpreted to have initiated by shear across set 3 joints. The Opal Mound fault is oriented subparallel to set 2 joints. Its west-side-up slip sense is consistent with it playing a role in rolling-hinge deformation in the footwall of the basin-bounding fault. The Negro Mag fault is oriented subparallel to set 1 joints and it appears to accommodate south-side-up displacement. The substantial majority of Pleistocene rhyolite was erupted on the upthrown side of the Negro Mag fault. These relations suggest the speculation that the Negro Mag fault represents the northern boundary of an unexposed bysmalith that could be interpreted to represent continued growth of the batholith into Quaternary time.

ACKNOWLEDGMENTS

Fieldwork in the Mineral Mountains that forms the basis of this report was supported by DOE contract DE-EE0007080. Drew Coleman shared unpublished fracture data from his Ph.D. dissertation. Discussions with members of the FORGE team, particularly Stefan Kirby, Emily Kleber, Stuart Simmons, Kris Pankow, and Rick Allis were invaluable in the development of the ideas presented here. The resulting paper benefitted from constructive reviews by Stuart Simmons, Stefan Kirby, and Drew Coleman.

REFERENCES

Anderson, E.M., 1951, The dynamics of faulting and dyke formation with applications to Britain (2nd edition): Edinburgh, Oliver and Boyd.

Axen, G.J., and Bartley, J.M., 1997, Field tests of rolling hinges: Existence, mechanical types, and implications for extensional tectonics: Journal of Geophysical Research, v. 102, No. B9, p. 20,515–20,537.

Axen, G.J., Bartley, J.M., and Selverstone, J., 1995, Structural expression of a rolling hinge in the footwall of the Brenner Line normal fault, eastern Alps: Tectonics, v. 14, p. 1380–1392.

Bartley, J.M., Fletcher, J.M., and Glazner, A.F., 1990, Tertiary extension and contraction of lower-plate rocks in the central Mojave metamorphic core complex: Tectonics, v. 9, p. 521–534.

Buck, W.R., 1988, Flexural rotation of normal faults: Tectonics, v. 7, p. 959–973.

Coleman, D.S., 1991, Geology of the Mineral Mountains batholith, Utah [unpublished Ph.D. dissertation]: University of Kansas, Lawrence, Kansas, 219 p.

Coleman, D.S., Bartley, J.M., Walker, J.D., Price, D.E., and Friedrich, A.M., 1997, Extensional Faulting, Footwall Deformation and Plutonism in the Mineral Mountains, Southern Sevier Desert, *in* Link, P., and Kowallis, B., eds., Mesozoic to Recent geology of Utah (Field Trip Guidebook, 1997 GSA Annual Meeting): Brigham Young University Geology Studies, v. 42, part 2, p. 203–233.

Coleman, D.S., Gray, W., and Glazner, A.F., 2004, Rethinking the emplacement and evolution of zoned plutons: Geochronologic evidence for incremental assembly of the Tuolumne Intrusive Suite, California: Geology, v. 32, p. 433–436.

Coleman, D.S., and Walker, J.D., 1994, Modes of tilting during extensional core complex development: Science, v. 263, p. 215–218.

Coleman, D.S., Walker, J.D., Bartley, J.M., and Hodges, K.V., 2001, Thermochronologic evidence for footwall deformation during extensional core complex development, Mineral Mountains, Utah, *in* Erskine, M., Bartley, J.M., Faulds, J., and Rowley, P.D., editors, The Geologic Transition—Colorado Plateau to Basin and Range: Guidebook - Pacific Section, American Association of Petroleum Geologists, vol. 78, p. 155–168.

Hamblin, W.K., 1965, Origin of "reverse drag" on the downthrown side of normal faults: Geological Society of America Bulletin, v. 76, p. 1145–1164.

Hardwick, C., Hurlbut, W., and Gwynn, M., 2019, Geophysical surveys of the Milford, Utah, FORGE site—gravity and TEM, *in* Allis, R., and Moore, J.N., editors, Geothermal characteristics of the Roosevelt Hot Springs system and adjacent FORGE EGS site, Milford, Utah: Utah Geological Survey Miscellaneous Publication 169-F, 15 p., https://doi.org/10.34191/MP-169-F.

Hintze, L.F., Willis, G.C., Laes, D.Y.M., Sprinkel, D.A., and Brown, K.D., 2000, Digital Geologic Map of Utah: Utah Geologic Survey, Map 179DM, 1:500,000 scale.

Kamb, W.B., 1959, Ice petrofabric observations from Blue Glacier, Washington, in relation to theory and experiment: Journal of Geophysical Research, v. 64, p. 1891–1909.

Knudsen, T., Kleber, E., Hiscock, A., and Kirby, S.M., 2019, Quaternary geology of the Utah FORGE site and vicinity, Millard and Beaver Counties, Utah, *in* Allis, R., and Moore, J.N., editors, Geothermal characteristics of the Roosevelt Hot Springs system and adjacent FORGE EGS site, Milford, Utah: Utah Geological Survey Miscellaneous Publication 169-B, 21 p., 2 appendices, https://doi.org/10.34191/MP-169-B.

Manning, A.M., and Bartley, J.M., 1994, Post-mylonitic deformation in the Raft River metamorphic core complex, northwest Utah: Evidence for a rolling hinge: Tectonics, v. 13, p. 596–612.

Machette, M.N., Steven, T.A., Cunningham, C.G., and Anderson, J.J., 1984, Geologic map of the Beaver Quadrangle, Beaver and Piute Counties, Utah: U. S. Geological Survey Miscellaneous Investigations, Map I-1520, scale 1:50,000.

Michel, J., Baumgartner, L., Putlitz, B., Schaltegger, U., and Ovtcharova, M., 2008, Incremental growth of the Patagonian Torres del Paine laccolith over 90 k.y.: Geology, v. 36, n. 6, p. 459–462.

Miller, J., Allis, R., and Hardwick, C., 2019, Interpretation of seismic reflection surveys near the FORGE enhanced geothermal systems site, Utah, in Allis, R., and Moore, J.N., editors, Geothermal characteristics of the Roosevelt Hot Springs system and adjacent FORGE EGS site, Milford, Utah: Utah Geological Survey Miscellaneous Publication 169-H, 13 p., https://doi.org/10.34191/MP-169-H.

Nielson, D.L., Evans, S.H., Jr., and Sibbett, B.S., 1986, Magmatic, structural, and hydrothermal evolution of the Mineral Mountains intrusive complex, Utah: Geological Society of America Bulletin, v. 97, p. 765–777.

Price, D.E, 1998, Timing, magnitude, and three-dimensional structure of detachment-related extension, Mineral Mountains, Utah [unpublished M.S. thesis]: University of Utah, Salt Lake City, 67 p.

Proffett, J.M., Jr., 1977, Cenozoic geology of the Yerington District, Nevada, and implications for the nature and origin of Basin and Range faulting: Geological Society of America Bulletin, v. 88, p. 247–266.

Sibbett, B.S., and Nielson, D.L., 2017, Geologic map of the central Mineral Mountains, Beaver County, Utah: Utah Geological Survey Miscellaneous Publication 17-2DM.

Smith, R.B., and Bruhn, R.L., 1984, Intraplate extensional tectonics of the eastern Basin-Range: inferences on the structural style from seismic reflection data, regional tectonics, and thermal-mechanical models of brittle-ductile deformation: Journal of Geophysical Research, v. 89, p. 5733–5762.

Spencer, J.E., 1984, Role of tectonic denudation in warping and uplift of low-angle normal faults: Geology, v. 12, p. 95–98.

Thatcher, W., and Hill, D.P., 1991, Fault orientations in extensional and conjugate strike-slip environments and their implications: Geology, v. 19, p. 1116–1120.

Wernicke, B.P., and Axen, G.J., 1988, On the role of isostasy in the evolution of normal fault systems: Geology, v. 16, p. 848–851.

Wills, S., and Buck, W.R., 1997, Stress-field rotation and rooted detachment faults; a Coulomb failure analysis: Journal of Geophysical Research, v. 102, p. 20,503–20,514.